

Relaxed Wasserstein with Applications to GANs

Xin Guo ^{*} Johnny Hong [†] Tianyi Lin [‡] Nan Yang [§]

May 19, 2017

Abstract

We propose a novel class of statistical divergences called *Relaxed Wasserstein* (RW) divergence. RW divergence generalizes Wasserstein distance and is parametrized by strictly convex, differentiable functions. We establish for RW several key probabilistic properties, which are critical for the success of Wasserstein distances. In particular, we show that RW is dominated by Total Variation (TV) and Wasserstein- L^2 distance, and establish continuity, differentiability, and duality representation of RW divergence. Finally, we provide a non-asymptotic moment estimate and a concentration inequality for RW divergence.

Our experiments on image generation problems show that RWGANs with Kullback-Leibler (KL) divergence provide competitive performance compared with many state-of-the-art approaches. Empirically, we show that RWGANs possess better convergence properties than WGANs, with competitive inception scores. In comparison to the existing literature in GANs, which are ad-hoc in the choices of cost functions, this new conceptual framework not only provides great flexibility in designing general cost functions, e.g., for applications to GANs, but also allows different cost functions implemented and compared under a unified mathematical framework.

1 Introduction

GANs. Generative Adversarial Networks (GANs) [16] provide a versatile class of models for generative modeling. Since its introduction to the machine learning community, the GAN framework has become a popular approach for numerous applications. Examples include high resolution image generation [12, 32], image inpainting [38], image super-resolution [21], visual manipulation [40], text-to-image synthesis [33], video generation [37], semantic segmentation [23], and abstract reasoning diagram generation [15]. Some analysis has been conducted to establish the theoretical justifications of GANs, such as [2]. For Bayesian and dynamical interpretations of GANs, see [22, 26].

^{*}Department of Industrial Engineering and Operations Research, University of California, Berkeley, USA. Email: xin-guo@berkeley.edu.

[†]Department of Statistics, University of California, Berkeley, USA. Email: jcyhong@berkeley.edu.

[‡]Department of Industrial Engineering and Operations Research, University of California, Berkeley, USA. Email: darren_lin@berkeley.edu.

[§]Department of Industrial Engineering and Operations Research, University of California, Berkeley, USA. Email: nanyang@berkeley.edu.

The core idea in GANs is to formulate the generative modeling problem as a competing game between two networks: a generator network and a discriminator network. The generator attempts to fool the discriminator by converting random noise into sample data, while the discriminator tries to identify whether the input sample is a generated data sample or a true data sample. While the basic premise of GANs is straightforward and intuitive, the training of GANs poses great computational challenges.

Many extensions and modifications have been proposed to address the computational issues. LSGANs [25] utilize the least squares loss function for the discriminator, instead of the sigmoid cross entropy loss function. Empirically, LSGANs are shown to generate higher quality images than regular GANs, and have a more stable performance during the learning process. DRAGAN [20] is an algorithm developed to address the issue that the GAN training, which involves simultaneous gradient descent, lacks a clear game-theoretic justification. The key idea behind the DRAGAN algorithm is to introduce regret minimization as a technique to reach equilibrium in games. Consequently DRAGAN justifies the success of simultaneous gradient descent in GANs. CGANs [28] are the conditional version of GANs. They address the issue that there is no control on modes of the data being generated in an unconditioned generative model and stabilize the training. InfoGANs [10] are an information-theoretic extension to GANs. They encourage interpretable and meaningful representations, by maximizing the mutual information between a fixed small subset of the GAN’s noise variables and the observations. They are shown to discover highly semantic and meaningful hidden representations on a number of image datasets. ACGANs [30] improve GANs by adding more structure to the GAN latent space along with a specialized cost function. This modification results in higher quality samples. In addition, it provides new analysis for assessing the discriminability and diversity of samples from class-conditional image synthesis models. EBGANs [39] are based on an energy-based formulation for GANs. The idea is to view the discriminator as an energy function that attributes low energies to the regions near the data manifold and higher energies to other regions. Furthermore, the EBGAN framework is demonstrated to generate reasonable high-resolution images without a multi-scale approach. BEGANs [5] adopt a new equilibrium enforcing method paired with a loss derived from the Wasserstein distance to train auto-encoder based GANs. This approach balances the generator and discriminator during training. Additionally, it provides a new approximate convergence measure, fast and stable training, and high visual quality.

WGANs. A recurring theme to improve the GANs training process is the choice of cost functions. The first proposed class of cost functions is based on the Jensen-Shannon (JS) divergence, which is essentially a symmetrized version of the Kullback-Leibler (KL) divergence [16]. [1] shows that JS divergence has undesirable properties that contribute to difficulties in training GANs. Instead, [1] proposes Wasserstein GAN (WGAN) as an alternative. In particular, WGANs choose the Earth Mover (EM) distance, also known as Wasserstein- L^1 distance, for the cost function. Wasserstein distance is commonly used to measure closeness of two probability distributions; for example, in optimal transport theory [36]. It is shown to be dominated by the Total Variation (TV) distance, a desirable probabilistic property for a statistical divergence.

GANs with Wasserstein- L^1 distance possess superior theoretical properties compared to the standard GANs with the JS divergence [1]. In particular, the choice of Wasserstein- L^1 distance leads to continuity,

differentiability and duality of the cost function, which allows for gradient computation in the corresponding optimization problem. Empirically, the use of Wasserstein- L^1 distance not only improves learning stability and avoids the issue of mode collapse, but also provides meaningful learning curves that can be used for debugging and hyperparameter search purposes. To enforce a Lipschitz constraint in the optimization procedure, clamping, or weight clipping, is proposed in [1]. Recently, gradient penalty is proposed to further improve the training stability [17].

Our work. We propose a novel class of statistical divergence called *Relaxed Wasserstein* (RW) divergence. RW divergence is Wasserstein distance parametrized by strictly convex, differentiable functions. This provides great flexibility in designing general cost functions; for example, for applications to GANs. In order to demonstrate that RW divergence is a viable option for comparing probability distributions and is superior to the particular choice of Wasserstein distance, there are critical theoretical questions and computations issues to be resolved.

- Does RW have sufficient smoothness property to allow the computation of gradient in the optimization procedure?
- As a statistical divergence, how does RW compare with the Wasserstein distance and other divergences?
- How does RW compare with the Wasserstein distance and other divergences, when used in GANs?

We first establish that RW is dominated by TV and squared Wasserstein- L^2 (Theorem 3.1). In addition, we provide a nonasymptotic moment estimate and a concentration inequality for RW divergence (Theorem 3.2 and 3.3). In order to further show that RW divergence is a reasonable choice for applications to GANs, we then prove continuity and differentiability demonstrating the existence of gradient (Theorem 3.5). This property allow for gradient descent based optimization procedure for GANs as shown in [1]. We then establish a decomposition of RW in terms of distorted squared Wasserstein- L^2 distance with correction terms (Lemma 3.4). With further exploitation of duality, this result leads to an explicit formula for gradient computation, and suggests the use of asymmetric clamping in the training procedure, akin to clamping in [1].

We study the empirical performance of RW divergence in image generation problems and compare it with many state-of-the-art approaches for GANs. We specialize our numerical studies on RWGANs with KL divergence. Using MNIST and Fashion-NIST datasets, our numerical studies with the DCGAN architecture show that RWGANs provide competitive performance compared to the popular approaches, suggesting that RWGANs are indeed a viable alternative. To further investigate the empirical properties of RWGANs, we compare RWGANs’ training performance on CIFAR-10 and ImageNet datasets with WGANs and WGANs with gradient penalty (WGAN-GP). Our experiments suggest that RWGANs illustrate a tradeoff between WGANs and WGANs-GP. While WGANs-GP achieve the fastest training among the three approaches, it might fail to converge in certain applications. Meanwhile, RWGANs achieve faster training compared to WGANs, with comparable convergence behaviors. On the other hand, RWGANs achieve the highest inception scores, a performance measure which was found to correlate well with human evaluations [34], during the initial stage of training with CIFAR-10 for both DCGAN and MLP architecture. For WGANs, [1] cautions against the use of weight clipping, but our experiments demonstrate the potential benefit of

weight clipping when a suitable choice of clipping is made.

Open question. Theoretically, this new conceptual framework under RW provides a unified mathematical framework to implement and compare different cost functions. The flexibility in RW divergence raises a natural question on how to select the underlying convex function ϕ for a given problem. Empirically, how to select ϕ consistently in a robust way remains an open problem.

While the main focus of this paper is applications to GANs, we believe that the theoretical results of RW divergence can be a valuable addition to the rich theory for optimal transport, where regularities of Wasserstein-based cost functions have been extensively studied (for example, [7, 8], [9] and [36]).

Organization of the paper. The rest of the paper is organized as follows. Section 2 provides the preliminaries and notations that will be used throughout the paper. Section 3 describes the RW divergence and discusses its theoretical properties. In Section 4, we discuss the implementation of the method and present two numerical studies on real data examples. Section 5 concludes our paper.

2 Background

In this section, we will review definitions and relevant properties of Bregman divergence and Wasserstein distance.

2.1 Notations

Throughout the paper, the following notations are used unless otherwise stated.

\mathcal{X} and \mathcal{Y} denote compact sets in \mathbb{R}^d , with $D = D(\mathcal{X}) = \max_{x_1, x_2 \in \mathcal{X}} \|x_1 - x_2\|_2$ being the diameter of \mathcal{X} . \mathbb{P}_r denotes an unknown true probability distribution and $\{\mathbb{P}_\theta : \theta \in \mathbb{R}^d\}$ is a parametric family of probability measures defined on \mathcal{X} .

\mathbb{P} and \mathbb{Q} denote probability distributions, $\mathcal{P}(\mathcal{X})$ denotes the set of probability distributions defined on \mathcal{X} , and $\Pi(\mathbb{P}, \mathbb{Q})$ denotes the set of all couplings of \mathbb{P} and \mathbb{Q} , i.e., the set of all joint distributions over $\mathcal{X} \times \mathcal{X}$ with marginal distributions being \mathbb{P} and \mathbb{Q} .

The Total Variation distance between \mathbb{P} and \mathbb{Q} is denoted as $\|\mathbb{P} - \mathbb{Q}\|_{TV} := \inf_{\pi \in \Pi(\mathbb{P}, \mathbb{Q})} \pi(X \neq Y)$.

$D_\phi(p, q)$, the Bregman divergence between two vectors $p, q \in \mathbb{R}^d$, is defined as $D_\phi(p, q) = \phi(p) - \phi(q) - \langle \nabla \phi(q), p - q \rangle$, for any given differentiable and strictly convex function ϕ . The same notation $D_\phi(\cdot, \cdot)$ is used for Bregman divergence between the continuous probability distributions \mathbb{P} and \mathbb{Q} , as in [18]: $D_\phi(\mathbb{P}, \mathbb{Q}) = \int_{\mathcal{X}} \left[\phi\left(\frac{d\mathbb{P}}{d\mathbb{S}}\right) - \phi\left(\frac{d\mathbb{Q}}{d\mathbb{S}}\right) - \left\langle \nabla \phi\left(\frac{d\mathbb{Q}}{d\mathbb{S}}\right), \frac{d\mathbb{P}}{d\mathbb{S}} - \frac{d\mathbb{Q}}{d\mathbb{S}} \right\rangle \right] d\mathbb{S}$, where \mathbb{P} and \mathbb{Q} are absolutely continuous with respect to \mathbb{S} .

2.2 Wasserstein Distance

Definition 2.1. *The Wasserstein distance of order p between the probability distributions \mathbb{P} and \mathbb{Q} is defined as*

$$W_p(\mathbb{P}, \mathbb{Q}) = \left(\inf_{\pi \in \Pi(\mathbb{P}, \mathbb{Q})} \int_{\mathcal{X} \times \mathcal{X}} [m(x, y)]^p d\pi(x, y) \right)^{1/p},$$

where $p \in [1, \infty)$, and m is a metric on \mathcal{X} .

For the d -dimensional Euclidean space $\mathcal{X} = \mathbb{R}^d$, a natural choice is the L^q -distance $m(x, y) = \|x - y\|_q$ with $q \geq 1$. This defines the Wasserstein- L_q distance of order p :

$$W_{L^q}(\mathbb{P}, \mathbb{Q}) = \left(\inf_{\pi \in \Pi(\mathbb{P}, \mathbb{Q})} \int_{\mathcal{X} \times \mathcal{X}} \|x - y\|_q^p d\pi(x, y) \right)^{1/p}. \quad (1)$$

Another example is the squared Wasserstein- L_2 distance of order 2: $W_{L^2}(\mathbb{P}, \mathbb{Q})^2 = \int_{\mathcal{X}} \|x\|_2^2 d\mathbb{P} + \int_{\mathcal{X}} \|y\|_2^2 d\mathbb{Q} - 2 \sup_{\pi \in \Pi(\mathbb{P}, \mathbb{Q})} \mathbb{E}_{\pi} [\langle X, Y \rangle]$, where (X, Y) are random variables with a joint distribution π .

For any two distributions \mathbb{P} and \mathbb{Q} , $W(\mathbb{P}, \mathbb{Q})$ is non-negative and equals zero if and only if $\mathbb{P} = \mathbb{Q}$ almost everywhere. Wasserstein distance is a metric since it is symmetric and satisfies the triangle inequality.

2.3 Bregman Divergence

Definition 2.2. *For two vectors x and y in \mathbb{R}^d and a strictly convex function $\phi(x) : \mathbb{R}^d \rightarrow \mathbb{R}$, the Bregman divergence is defined as*

$$D_{\phi}(x, y) = \phi(x) - \phi(y) - \langle \nabla \phi(y), x - y \rangle.$$

Examples of loss functions and their associated Bregman divergences include

- L^2 loss: $D_{\phi}(x, y) = \|x - y\|_2^2$, where $\phi(x) = \|x\|_2^2$,
- Itakura-Saito divergence: $D_{\phi}(x, y) = x/y - \log(x/y) - 1$, where $\phi(x) = -\log x$,
- KL divergence: $D_{\phi}(x, y) = \sum_{i=1}^d x_i \log(x_i/y_i)$, where $\phi(x) = \sum_{i=1}^d x_i \log x_i$,
- Mahalanobis distance: $D_{\phi}(x, y) = (x - y)^T A (x - y)$, where $\phi(x) = x^T A x$, A is a strictly positive definite matrix.

As a divergence function, $D_{\phi}(x, y)$ is always nonnegative by the convexity of ϕ . $D_{\phi}(x, y) = 0$ if and only if $x = y$. However, it may not be a metric because it may not be symmetric, and it may not satisfy the triangle inequality. In [31], they show an asymptotic equivalence between f -divergences (in particular, χ^2 -divergence) and Bregman divergences under some conditions. In [4], they show that conditional expectation is the optimal predictor for all Bregman divergences. Moreover, Bregman divergences are the only class of such loss functions. This property ensures the convergence of k -means algorithm when Bregman divergence is used as a loss function.

3 Relaxed Wasserstein (RW) Divergence

We propose a novel class of statistical divergence called Relaxed Wasserstein (RW) divergences, which can be seen as a combination of Bregman divergence [3] and Wasserstein distance. The term *relaxed* is used because it relaxes the L^2 distance to a broader class of nonsymmetric divergences. We then analyze theoretical properties of RW divergence.

Definition 3.1. *The Relaxed Wasserstein (RW) divergence between the probability distributions \mathbb{P} and \mathbb{Q} is defined as*

$$W_{D_\phi}(\mathbb{P}, \mathbb{Q}) = \inf_{\pi \in \Pi(\mathbb{P}, \mathbb{Q})} \int_{\mathcal{X} \times \mathcal{X}} D_\phi(x, y) d\pi(x, y), \quad (2)$$

where D_ϕ is the Bregman divergence corresponding to a smooth and strictly convex function $\phi : \mathbb{R}^d \rightarrow \mathbb{R}$.

Similar to Wasserstein distance, RW divergence is non-negative and equals zero if and only if $\mathbb{P} = \mathbb{Q}$ almost everywhere. However, RW is usually asymmetric.

Remark 1. *Bregman divergence includes two important special cases: L^2 distance and KL divergence. Setting $\phi(x) = \|x\|_2^2$, then $D_\phi(x, y) = \|x - y\|_2^2$, and $W_{D_\phi} = W_{L^2}^2$. Setting $\phi(x) = -\sum_{i=1}^d x_i \log x_i$ gives the KL divergence between vectors x and y in \mathcal{X} , and $W_{D_\phi} = W_{KL}$ is the RW divergence with KL.*

Besides Wasserstein distances, Total Variation (TV) is another classical notion of distance between probability distributions. It has been shown that Wasserstein distances are controlled by weighted TV (Theorem 6.15 in [36]). The following theorem establishes the relationship among RW divergence, TV, and the Wasserstein- L^2 distance of order 2. Specifically, the RW divergence is dominated by the TV and the squared Wasserstein distance of order 2.

Theorem 3.1. *(Domination by Total Variation distance and Wasserstein- L^2 distance) Let ϕ be a differentiable, strictly convex function with L -Lipschitz gradients¹. Then the corresponding RW divergence W_{D_ϕ} satisfies the following two inequalities for all probability distributions \mathbb{P} and \mathbb{Q} on a compact set $\mathcal{X} \subset \mathbb{R}^d$:*

1. $W_{D_\phi}(\mathbb{P}, \mathbb{Q}) \leq 2LD^2 \|\mathbb{P} - \mathbb{Q}\|_{TV}$, where D is the diameter of \mathcal{X} ;
2. $W_{D_\phi}(\mathbb{P}, \mathbb{Q}) \leq \frac{L}{2} W_{L^2}(\mathbb{P}, \mathbb{Q})^2$.

Proof. For 1., define π as the transference plan obtained by keeping all the mass shared by \mathbb{P} and \mathbb{Q} fixed, and distributing the rest uniformly so that $\pi(dx, dy) = (\mathbb{P} \wedge \mathbb{Q})(dx) \delta_{\{y=x\}} + \frac{1}{a}(\mathbb{P} - \mathbb{Q})_+(dx)(\mathbb{P} - \mathbb{Q})_-(dy)$,

¹We say a function ϕ has L -Lipschitz gradients if $\|\nabla\phi(x) - \nabla\phi(y)\| \leq L\|x - y\|$ for all $x, y \in \mathcal{X}$.

where $\mathbb{P} \wedge \mathbb{Q} = \mathbb{P} - (\mathbb{P} - \mathbb{Q})_+$ and $a = (\mathbb{P} - \mathbb{Q})_+[\mathcal{X}] = (\mathbb{P} - \mathbb{Q})_-[\mathcal{X}]$. Then

$$\begin{aligned}
& W_{D_\phi}(\mathbb{P}, \mathbb{Q}) \\
& \leq \int_{\mathbb{R}^d \times \mathbb{R}^d} D_\phi(x, y) \pi(dx, dy) \\
& = \frac{1}{a} \int_{\mathbb{R}^d \times \mathbb{R}^d} [\phi(x) - \phi(y) - \langle \nabla \phi(y), x - y \rangle] (\mathbb{P} - \mathbb{Q})_+(dx) (\mathbb{P} - \mathbb{Q})_-(dy) \\
& = \frac{1}{a} \int_{\mathbb{R}^d \times \mathbb{R}^d} \left[\int_0^1 \langle \nabla \phi(tx + (1-t)y) - \nabla \phi(y), x - y \rangle dt \right] (\mathbb{P} - \mathbb{Q})_+(dx) (\mathbb{P} - \mathbb{Q})_-(dy) \\
& \leq \frac{L}{a} \int_{\mathbb{R}^d \times \mathbb{R}^d} \left[\|x - y\|_2^2 \left(\int_0^1 t dt \right) \right] (\mathbb{P} - \mathbb{Q})_+(dx) (\mathbb{P} - \mathbb{Q})_-(dy) \\
& \leq \frac{L}{a} \int_{\mathbb{R}^d \times \mathbb{R}^d} \left[\|x - x_0\|_2^2 + \|x_0 - y\|_2^2 \right] (\mathbb{P} - \mathbb{Q})_+(dx) (\mathbb{P} - \mathbb{Q})_-(dy) \\
& \leq L \left[\int_{\mathbb{R}^d \times \mathbb{R}^d} \|x - x_0\|_2^2 (\mathbb{P} - \mathbb{Q})_+(dx) + \int_{\mathbb{R}^d \times \mathbb{R}^d} \|x_0 - y\|_2^2 (\mathbb{P} - \mathbb{Q})_-(dy) \right] \\
& = L \int_{\mathbb{R}^d \times \mathbb{R}^d} \|x - x_0\|_2^2 |\mathbb{P} - \mathbb{Q}|(dx) \leq 2LD^2 \|\mathbb{P} - \mathbb{Q}\|_{TV}.
\end{aligned}$$

For 2., note that for $x, y \in \mathcal{X} \subset \mathbb{R}^d$,

$$\begin{aligned}
D_\phi(x, y) & = \langle \phi(x) - \phi(y) - \nabla \phi(y), x - y \rangle \\
& = \int_0^1 \langle \nabla \phi(tx + (1-t)y), x - y \rangle dt - \langle \nabla \phi(y), x - y \rangle \\
& = \int_0^1 \langle \nabla \phi(tx + (1-t)y) - \nabla \phi(y), x - y \rangle dt \leq \left(L \|x - y\|_2^2 \right) \int_0^1 t dt = \frac{L}{2} \|x - y\|_2^2.
\end{aligned}$$

Since for any coupling $\pi \in \Pi(\mathbb{P}, \mathbb{Q})$, π is a probability measure on $\mathbb{R}^d \times \mathbb{R}^d$ with marginals \mathbb{P} and \mathbb{Q} , $\pi(dx, dy) \geq 0$. The result follows by integrating both sides with respect to π and taking infimum. \square

Next, we state the nonasymptotic moment estimates and the concentration inequalities for RW divergence. The two theorems follow by applying Theorem 1 and Theorem 2 from [14] to the right hand side of Theorem 3.1.2. Let $\mathbb{P}_r \in \mathcal{P}(\mathbb{R}^d)$ and let \mathbb{P}_n be the empirical distribution based on n observations from \mathbb{P}_r . Let L be the Lipschitz constant of $\nabla \phi$. Define $M_q(\mathbb{P}_r) = \int_{\mathcal{X}} \|x\|_2^q d\mathbb{P}_r$ and $\mathcal{E}_{\alpha, \pi}(\mathbb{P}_r) = \int_{\mathcal{X}} e^{\gamma \|x\|_2^\alpha} d\mathbb{P}_r$.

Theorem 3.2. (*Moment estimate of RW divergence*) Assume that $M_q(\mathbb{P}_r) < +\infty$ for some $q > 2$. Then there exists a constant $C(q, d) > 0$ such that, for $n \geq 1$,

$$\mathbb{E} [W_{D_\phi}(\mathbb{P}_n, \mathbb{P}_r)] \leq \frac{C(q, d) L M_q^{\frac{2}{q}}(\mathbb{P}_r)}{2} \cdot \begin{cases} n^{-\frac{1}{2}} + n^{-\frac{q-2}{q}}, & 1 \leq d \leq 3, q \neq 4, \\ n^{-\frac{1}{2}} \log(1+n) + n^{-\frac{q-2}{q}}, & d = 4, q \neq 4, \\ n^{-\frac{2}{d}} + n^{-\frac{q-2}{q}}, & d \geq 5, q \neq d/(d-2). \end{cases}$$

Theorem 3.3. (*Concentration of RW divergence*) Assume one of the three following conditions holds,

$$\exists \alpha > 2, \exists \gamma > 0, \mathcal{E}_{\alpha, \gamma}(\mathbb{P}_r) < \infty, \tag{3}$$

$$\text{or } \exists \alpha \in (0, 2), \exists \gamma > 0, \mathcal{E}_{\alpha, \gamma}(\mathbb{P}_r) < \infty, \tag{4}$$

$$\text{or } \exists q > 4, M_q(\mathbb{P}_r) < \infty. \tag{5}$$

Then for $n \geq 1$ and $\epsilon > 0$,

$$\text{Prob}(W_{D_\phi}(\mathbb{P}_n, \mathbb{P}_r) \geq \epsilon) \leq a(n, \epsilon)I_{\{\epsilon \leq \frac{L}{2}\}} + b(n, \epsilon),$$

where

$$a(n, \epsilon) = C_1 \begin{cases} e^{-\frac{4cn\epsilon^2}{L^2}}, & 1 \leq d \leq 3, \\ e^{-\frac{4cn\epsilon^2}{L^2} \log^2(2 + \frac{L}{2\epsilon})}, & d = 4, \\ e^{-cn(\frac{2\epsilon}{L})^{\frac{d}{2}}}, & d \geq 5, \end{cases}$$

and

$$b(n, \epsilon) = C_2 \begin{cases} e^{-cn(\frac{2\epsilon}{L})^{\frac{\alpha}{2}}} I_{\{\epsilon > \frac{L}{2}\}}, & \text{under condition (3),} \\ e^{-c(\frac{2n\epsilon}{L})^{\frac{\alpha-\epsilon}{2}}} I_{\{\epsilon \leq \frac{L}{2}\}} + e^{-c(\frac{2n\epsilon}{L})^{\frac{\alpha}{2}}} I_{\{\epsilon > \frac{L}{2}\}}, & 0 < \epsilon < \alpha, \text{ under condition (4),} \\ n(\frac{2n\epsilon}{L})^{-\frac{q-\epsilon}{2}}, & 0 < \epsilon < q, \text{ under condition (5).} \end{cases}$$

Here c , C_1 , and C_2 are constants depending on q and d .

The following simple yet important lemma further decomposes the RW divergence in terms of the distorted squared Wasserstein- L_2 distance of order 2, with additional residual terms that do not depend on the choice of coupling π .

Lemma 3.4. (*Decomposition of RW divergence*) *The RW divergence admits the following decomposition:*

$$\begin{aligned} W_{D_\phi}(\mathbb{P}, \mathbb{Q}) &= \frac{1}{2} W_{L^2}(\mathbb{P}, \mathbb{Q} \circ (\nabla \phi)^{-1})^2 + \mathbb{E}_{X \sim \mathbb{P}}[\phi(X)] - \mathbb{E}_{Y \sim \mathbb{Q}}[\phi(Y)] + \mathbb{E}_{Y \sim \mathbb{Q}}[\langle \nabla \phi(Y), Y \rangle] \\ &\quad - \frac{1}{2} [\mathbb{E}_{X \sim \mathbb{P}}[\|X\|_2^2] + \mathbb{E}_{Y \sim \mathbb{Q} \circ (\nabla \phi)^{-1}}[\|Y\|_2^2]]. \end{aligned}$$

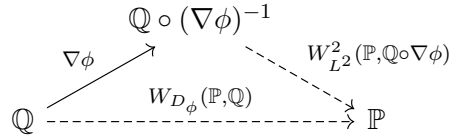


Figure 1: The decomposition of W_{D_ϕ} . The solid arrow denotes transformation. The dashed arrow denotes the distance between probability distributions.

Proof. Because ϕ is strictly convex, its gradient $\nabla \phi$ has a positive definite Jacobian matrix, which is also the Hessian of ϕ . Then by the inverse function theorem, $\nabla \phi$ is invertible. Denote its inverse with $(\nabla \phi)^{-1}$ and the composition of \mathbb{Q} and $(\nabla \phi)^{-1}$ as $\mathbb{Q} \circ (\nabla \phi)^{-1}$, then $\mathbb{E}_{Y \sim \mathbb{Q} \circ (\nabla \phi)^{-1}}[\|Y\|_2^2] = \mathbb{E}_{Y \sim \mathbb{Q}}[\|\nabla \phi(Y)\|_2^2]$.

Expanding $W_{D_\phi}(\mathbb{P}, \mathbb{Q})$ by the linearity of inner products yields

$$\begin{aligned}
W_{D_\phi}(\mathbb{P}, \mathbb{Q}) &= \inf_{\pi \in \Pi(\mathbb{P}, \mathbb{Q})} \int [\phi(x) - \phi(y) - \langle \nabla \phi(y), x - y \rangle] d\pi(x, y) \\
&= \mathbb{E}_{X \sim \mathbb{P}}[\phi(X)] - \mathbb{E}_{Y \sim \mathbb{Q}}[\phi(Y)] + \mathbb{E}_{Y \sim \mathbb{Q}}[\langle \phi(Y), Y \rangle] + \inf_{\pi \in \Pi(\mathbb{P}, \mathbb{Q})} \mathbb{E}_{X, Y \sim \pi}[\langle -\nabla \phi(Y), X \rangle] \\
&= \frac{1}{2} [\mathbb{E}_{X \sim \mathbb{P}}[\|X\|_2^2] + \mathbb{E}_{Y \sim \mathbb{Q}}[\|\nabla \phi(Y)\|_2^2] + \inf_{\pi \in \Pi(\mathbb{P}, \mathbb{Q})} \mathbb{E}_{X, Y \sim \pi}[\langle -2\nabla \phi(Y), X \rangle]] + \mathbb{E}_{X \sim \mathbb{P}}[\phi(X)] \\
&\quad - \mathbb{E}_{Y \sim \mathbb{Q}}[\phi(Y)] + \mathbb{E}_{Y \sim \mathbb{Q}}[\langle \nabla \phi(Y), Y \rangle] - \frac{1}{2} [\mathbb{E}_{X \sim \mathbb{P}}[\|X\|_2^2] + \mathbb{E}_{Y \sim \mathbb{Q}}[\|\nabla \phi(Y)\|_2^2]] \\
&= \frac{1}{2} W_{L^2}(\mathbb{P}, \mathbb{Q} \circ (\nabla \phi)^{-1})^2 + \mathbb{E}_{X \sim \mathbb{P}}[\phi(X)] - \mathbb{E}_{Y \sim \mathbb{Q}}[\phi(Y)] + \mathbb{E}_{Y \sim \mathbb{Q}}[\langle \nabla \phi(Y), Y \rangle] \\
&\quad - \frac{1}{2} [\mathbb{E}_{X \sim \mathbb{P}}[\|X\|_2^2] + \mathbb{E}_{Y \sim \mathbb{Q} \circ (\nabla \phi)^{-1}}[\|Y\|_2^2]].
\end{aligned}$$

□

The following theorem concerns continuity and differentiability of the parametrized RW divergence. The result is based upon the setup in [1]. Define a random variable Z with a fixed probability distribution $p(z)$ on \mathcal{Z} . Then define a parametric function $g_\theta : \mathcal{Z} \rightarrow \mathcal{X}$ to directly generate samples that follows a class of parametric probability distributions \mathbb{P}_θ . \mathbb{P}_θ is then used to approximate the unknown distribution \mathbb{P}_r .

Theorem 3.5. (*Continuity and differentiability of RW divergence*) *If g_θ is continuous in θ , then $W_{D_\phi}(\mathbb{P}_r, \mathbb{P}_\theta)$ is continuous in θ . If g_θ is locally Lipschitz with a constant $L(\theta, z)$ such that $\mathbb{E}[L(\theta, Z)^2] < \infty$ for all θ , then $W_{D_\phi}(\mathbb{P}_r, \mathbb{P}_\theta)$ is differentiable almost everywhere.*

Proof. Since ϕ and $\nabla \phi$ are differentiable, X and Y are defined on compact set \mathcal{X} , the correction terms in Lemma 3.4 are all continuous and differentiable with respect to θ . It suffices to show that $W_{L^2}(\mathbb{P}_r, \mathbb{P}_\theta)$ is almost everywhere differentiable. First, observe that for two vectors $\theta, \theta' \in \mathbb{R}^d$, let π be the joint distribution of $(g_\theta(Z), g_{\theta'}(Z))$ where $Z \sim p(z)$, then

$$W_{L^2}(\mathbb{P}_\theta, \mathbb{P}'_\theta) \leq [\mathbb{E}_{(X, Y) \sim \pi}[\|X - Y\|_2^2]]^{\frac{1}{2}} = [\mathbb{E}\|g_\theta(Z) - g_{\theta'}(Z)\|_2^2]^{\frac{1}{2}}.$$

The continuity of g_θ ensures that $\|g_\theta(Z) - g_{\theta'}(Z)\|^2 \rightarrow 0$ point-wise as $\theta \rightarrow \theta'$. Since \mathcal{X} is compact, $\|g_\theta(Z) - g_{\theta'}(Z)\|^2$ is uniformly bounded. Therefore by the bounded convergence theorem,

$$W_{L^2}(\mathbb{P}_\theta, \mathbb{P}'_\theta) \leq [\mathbb{E}\|g_\theta(Z) - g_{\theta'}(Z)\|_2^2]^{\frac{1}{2}} \rightarrow 0, \text{ as } \theta \rightarrow \theta'.$$

Hence by the triangle inequality, as $\theta \rightarrow \theta'$, $|W_{L^2}(\mathbb{P}_r, \mathbb{P}_\theta) - W_{L^2}(\mathbb{P}_r, \mathbb{P}_{\theta'})| \leq W_{L^2}(\mathbb{P}_\theta, \mathbb{P}'_\theta) \rightarrow 0$. This proves the continuity.

Now assume g_θ is locally Lipschitz, i.e., for each pair (θ, z) , there exists a constant $L(\theta, z)$ and an open neighborhood $N(\theta, z)$ around (θ, z) such that $\forall(\theta', z') \in N(\theta, z)$,

$$\|g_\theta(z) - g_{\theta'}(z')\|_2 \leq L(\theta, z)(\|\theta - \theta'\|_2 + \|z - z'\|_2).$$

By fixing $z' = z$ and taking expectation of squares of both sides, we get

$$\mathbb{E}\|g_\theta(Z) - g_{\theta'}(Z)\|_2^2 \leq \|\theta - \theta'\|_2^2 \mathbb{E}[L(\theta, Z)^2],$$

for all θ' in an open neighborhood of θ . Therefore,

$$|W_{L^2}(\mathbb{P}_r, \mathbb{P}_\theta) - W_{L^2}(\mathbb{P}_r, \mathbb{P}_{\theta'})| \leq W_{L^2}(\mathbb{P}_\theta, \mathbb{P}_{\theta'}) \leq [\mathbb{E}\|g_\theta(Z) - g_{\theta'}(Z)\|_2]^{\frac{1}{2}} \leq \|\theta - \theta'\|_2 \mathbb{E}[L(\theta, Z)^2]^{\frac{1}{2}},$$

i.e., $W_{L^2}(\mathbb{P}_r, \mathbb{P}_\theta)$ is locally Lipschitz and by Rademacher's theorem [13], is differentiable almost everywhere. \square

Note that a related version of this result has been proved in a different setting [24]. Our proof is simpler and exploits the intrinsic structure of RW divergence highlighted in Lemma 3.4.

In fact, this structure is also critical for establishing the following duality representation of RW divergence, combined with the following lemma modified from Theorem 3.1 in [6] for a compact set \mathcal{X} .

Lemma 3.6. (*Duality representation*) Suppose that two probability distributions \mathbb{P} and \mathbb{Q} satisfy

$$M(\mathbb{P}, \mathbb{Q}) := \frac{1}{2} \int_{\mathcal{X}} \|x\|_2^2 (d\mathbb{P} + d\mathbb{Q}) < +\infty. \quad (6)$$

Then there is a Lipschitz continuous solution $f : \mathcal{X} \rightarrow \mathbb{R}$ such that the squared Wasserstein- L_2 distance has a duality representation as

$$\frac{1}{2} W_{L^2}(\mathbb{P}, \mathbb{Q})^2 = \inf_{\pi \in \Pi(\mathbb{P}, \mathbb{Q})} \int_{\mathcal{X} \times \mathcal{X}} \frac{\|x - y\|_2^2}{2} d\pi = M(\mathbb{P}, \mathbb{Q}) - \left(\int_{\mathcal{X}} f d\mathbb{P} + \int_{\mathcal{X}} f^* d\mathbb{Q} \right),$$

where K is the Lipschitz constant of f and depends on \mathcal{X} , and f^* is defined as the conjugate of f so that $f^*(y) = \sup_{x \in \mathbb{R}^d} \{\langle x, y \rangle - f(x)\}$.

Theorem 3.7. (*Gradient computation*) Let \mathbb{P}_θ be the distribution of $g_\theta(Z)$ with Z being a random variable with distribution $p(z)$, assume g_θ is a locally Lipschitz function, and suppose that $M(\mathbb{P}_r, \mathbb{P}_\theta) < \infty$ as in (6). Then

1. $\nabla_\theta(\frac{1}{2} W_{L^2}(\mathbb{P}_r, \mathbb{P}_\theta)^2) = \mathbb{E}[g_\theta(Z) \nabla g_\theta(Z) - \nabla_\theta f(g_\theta(Z))]$.
2. There is a Lipschitz continuous solution $f : \mathcal{X} \rightarrow \mathbb{R}$ such that the gradient of the RW divergence $\nabla_\theta [W_{D_\phi}(\mathbb{P}_r, \mathbb{P}_\theta)]$ can be explicitly represented as

$$\nabla_\theta [W_{D_\phi}(\mathbb{P}_r, \mathbb{P}_\theta)] = \mathbb{E} [\nabla_\theta \phi(g_\theta(Z)) + \nabla_\theta \langle \phi(g_\theta(Z)), g_\theta(Z) \rangle + \nabla_\theta f(\nabla \phi(g_\theta(Z)))].$$

Proof. For 1., define $V(\tilde{f}, \theta) = \mathbb{E}_{\mathbb{P}_r} \left[\frac{\|X\|_2^2}{2} \right] + \mathbb{E}_{\mathbb{P}_\theta} \left[\frac{\|X\|_2^2}{2} \right] - \mathbb{E}_{\mathbb{P}_r}[\tilde{f}^*] - \mathbb{E}_{\mathbb{P}_\theta}[\tilde{f}]$. By Lemma 3.6, we know there exists a Lipschitz continuous function f such that $\frac{1}{2} W_{L^2}(\mathbb{P}_r, \mathbb{P}_\theta)^2 = V(f, \theta)$. Then by the Envelope theorem (for example, [27]) and Theorem 3.5, $\nabla_\theta(\frac{1}{2} W_{L^2}(\mathbb{P}_r, \mathbb{P}_\theta)^2) = \nabla_\theta V(f, \theta)$. Combined,

$$\begin{aligned} \nabla_\theta(\frac{1}{2} W_{L^2}(\mathbb{P}_r, \mathbb{P}_\theta)^2) &= \nabla_\theta \left(\mathbb{E}_{\mathbb{P}_\theta} \left[\frac{\|X\|_2^2}{2} \right] - \mathbb{E}[f(g_\theta(Z))] \right) = \nabla_\theta \mathbb{E} \left[\frac{g_\theta(Z)^2}{2} - f(g_\theta(Z)) \right] \\ &= \mathbb{E}[g_\theta(Z) \nabla_\theta g_\theta(Z) - \nabla_\theta f(g_\theta(Z))]. \end{aligned}$$

To prove 2., recall that $(X, Y) \sim \pi$, $X \sim \mathbb{P}_r$, $Y \sim \mathbb{P}_\theta$, $Z \sim p(z)$, and

$$\begin{aligned} W_{D_\phi}(\mathbb{P}_r, \mathbb{P}_\theta) &= \inf_{\pi \in \Pi(\mathbb{P}_r, \mathbb{P}_\theta)} \int [\phi(x) - \phi(y) - \langle \nabla \phi(y), x - y \rangle] d\pi(x, y) \\ &= \mathbb{E}[\phi(X)] - \mathbb{E}[\phi(Y)] + \mathbb{E}[\langle \phi(Y), Y \rangle] + \inf_{\pi \in \Pi(\mathbb{P}_r, \mathbb{P}_\theta)} \mathbb{E}[\langle X, -\nabla \phi(Y) \rangle]. \end{aligned}$$

Taking derivative with respect to θ ,

$$\nabla_\theta W_{D_\phi}(\mathbb{P}_r, \mathbb{P}_\theta) = -\nabla_\theta \mathbb{E}[\phi(Y)] + \nabla_\theta \mathbb{E}[\langle \phi(Y), Y \rangle] + \nabla_\theta \inf_{\pi \in \Pi(\mathbb{P}_r, \mathbb{P}_\theta)} \mathbb{E}_{X, Y \sim \pi}[\langle X, -\nabla \phi(Y) \rangle],$$

and by a direct calculation

$$\nabla_\theta \mathbb{E}[\phi(Y)] = \nabla_\theta \mathbb{E}[\phi(g_\theta(Z))] = \mathbb{E}[\nabla_\theta \phi(g_\theta(Z))], \nabla_\theta \mathbb{E}[\langle \phi(Y), Y \rangle] = \mathbb{E}[\nabla_\theta \langle \phi(g_\theta(Z)), g_\theta(Z) \rangle].$$

Let $\tilde{f} \in \arg \min_{f \in L^1, f \text{ Lipschitz}} [\int f^* d\mathbb{P}_r + \int f d\mathbb{P}_\theta]$ and the transformed random variable $Y' = -\nabla \phi(Y)$. Then by Lemma 3.6,

$$\begin{aligned} \nabla_\theta \inf_{\pi \in \Pi(\mathbb{P}_r, \mathbb{P}_\theta)} \mathbb{E}_{X, Y \sim \pi}[\langle -\nabla \phi(Y), X \rangle] &= \nabla_\theta \inf_{\pi \in \Pi(\mathbb{P}_r, \nabla(\phi(\mathbb{P}_\theta))} \mathbb{E}_{X, Y' \sim \pi}[\langle X, Y' \rangle] \\ &= \nabla_\theta \left[\int_{\mathbb{R}^d} \tilde{f}^* d\mathbb{P}_r + \int_{\mathbb{R}^d} \tilde{f} d\nabla \phi(\mathbb{P}_\theta) \right] \\ &= \nabla_\theta \int_{\mathbb{R}^d} \tilde{f} d\nabla \phi(\mathbb{P}_\theta) = \nabla_\theta \int_{\mathbb{R}^d} \tilde{f} (\nabla \phi(g_\theta(z))) dp(z) \\ &= \mathbb{E} \left[\nabla_\theta \tilde{f} (\nabla \phi(g_\theta(Z))) \right]. \end{aligned}$$

□

4 Empirical Results

In this section, we will present numerical evaluation on image generation to demonstrate the effectiveness and efficiency of using RW in GANs. We will first describe our approach of RW in GANs (RWGANs) and the experimental setting (Section 4.1), and then report the experimental results under RWGANs and other nine well-established variants of GANs (Section 4.2).

4.1 Experimental Approach and Setting

RWGANs approach. Recall that the goal of GANs is to estimate a probability distribution \mathbb{P}_r from the data. One first defines a random variable Z with a fixed distribution $p(z)$, then passes it through a parametric function $g_\theta : Z \rightarrow X$ to form a distribution \mathbb{P}_θ , in order to generate samples. By adapting θ , one can approximate the real distribution \mathbb{P}_r by \mathbb{P}_θ . This approximation is done by finding a solution f that optimizes a given cost function between \mathbb{P}_r and \mathbb{P}_θ .

In general it is intractable to derive an explicit solution for such an f , as seen from Theorem 3.7. Nevertheless, since the Wasserstein distance is parametrized by any convex function in RWGANs, it provides a great deal of flexibility in the choice of cost functions. For instance, one can choose an appropriate cost function such that $\nabla_\theta [W_{D_\phi}(\mathbb{P}_r, \mathbb{P}_\theta)]$ can be approximated by $\mathbb{E}_{Z \sim p(z)} [\nabla_\theta f(\nabla \phi(g_\theta(Z)))]$. This is the key idea in our experiments, where we choose to use the Kullback-Leibler divergence.

Experimental framework. Our experimental framework is similar to the one in WGANs [1] in that a) we apply back-propagation to train generative and discriminative models, and b) we update the parameters once in the generative model and n_{critic} times in the discriminative model.

Our framework differs from the one in WGANs [1] in several aspects. First, we use $\nabla\phi$ to do the asymmetric clamping instead of the symmetric clamping. Note that the asymmetric clamping guarantees the Lipschitz continuity of f and $\nabla\phi(w) \in [-c, c]$. Second, we use a scaling parameter S to stabilize the asymmetric clamping. This is critical for the experiment. Finally, we adopt RMSProp [35] instead of ADAM [19], that allows a choice of a larger step-size and further avoids the non-stationary problem reported in [29].

We describe our method with default parameters in Algorithm 1.

Algorithm 1 RWGANs. The default values $\alpha = 0.0005$, $c = 0.005$, $S = 0.01$, $m = 64$, $n_{critic} = 5$.

Require: α : the learning rate; c : the clipping parameter; m : the batch size; n_{critic} , the number of iterations of the critic per generator iteration; N_{max} , the maximum number of one forward pass and one backward pass of all the training examples.

Require: w_0 , initial critic parameters; θ_0 : initial generator’s parameters.

```

for  $N = 1, 2, \dots, N_{max}$  do
  for  $t = 0, \dots, n_{critic}$  do
    Sample a batch of real data  $\{x_i\}_{i=1}^m$  from  $\mathbb{P}_r$ .
    Sample a batch of prior samples  $\{z_i\}_{i=1}^m$  from  $p(z)$ .
     $g_w \leftarrow \frac{1}{m} \sum_{i=1}^m [\nabla_w f_w(x_i) - \nabla_w f_w(g_\theta(z_i))]$ .
     $w \leftarrow w + \alpha \cdot \text{RMSProp}(w, g_w)$ .
     $w \leftarrow \text{clip}(w, -S \cdot (\nabla\phi)^{-1}(-c), S \cdot (\nabla\phi)^{-1}(c))$ .
  end for
  Sample a batch of prior samples  $\{z_i\}_{i=1}^m$  from  $p(z)$ .
   $g_\theta \leftarrow -\frac{1}{m} \sum_{i=1}^m \nabla_\theta f_w(g_\theta(z_i))$ .
   $\theta \leftarrow \theta - \alpha \cdot \text{RMSProp}(\theta, g_\theta)$ .
end for

```

Experimental setting. In order to test RWGANs, we adopt nine baseline methods as discussed in the introduction. They are RWGANs, WGANs [1], WGANs-GP [17], CGANs [28], InfoGANs [10], GANs [16], LSGANs [25], DRAGANs [20], BEGANs [5], EBGANs [39], and ACGANs [30]. The implementation of all these approaches is based on publicly available online information². In addition, we use the following four standard and well-known datasets in our experiment.

1. MNIST³ is a dataset of handwritten digits. It has a training set of 60,000 examples, and a test set of 10,000 examples. It is a subset of a larger set available from NIST. The digits have been size-normalized and centered in a fixed-size image.

²<https://github.com/zmxlwm/pytorch-generative-model-collections>

³<http://yann.lecun.com/exdb/mnist/>

2. **Fashion-MNIST**⁴ is an alternative dataset of Zalando’s article images to **MNIST**. It consists of a training set of 60,000 examples and a test set of 10,000 examples. Each example is a 28×28 gray-scale image, associated with a label from 10 classes.
3. The **CIFAR-10**⁵ dataset consists of 60000 32×32 color images in 10 classes, with 6000 images per class. There are 50000 training images and 10000 test images.
4. The **ImageNet**⁶ dataset is a large visual database designed for visual object recognition software research. As of 2016, over ten million URLs of images have been hand-annotated by **ImageNet** to indicate which objects are picture. In at least one million of the images, bounding boxes are also provided.

Metric. The negative critic loss, well-known as the standard quantitative metric, is used in all our experiments. In addition to the negative critic loss, we use the inception score [34] to evaluate samples generated by three WGANs methods on **CIFAR-10** and **ImageNet**. The inception score is defined as follows:

$$\text{Inception_Score} = \exp \{ \mathbb{E}_{\mathbf{x}} [D_{\text{KL}}(p(y|\mathbf{x}), p(y))] \},$$

where $p(y|\mathbf{x})$ is given by the inception network, and high inception score is an indicator that the images generated by the model are highly interpretable and diversified. It is also highly correlated with human evaluation of the images.

4.2 Experimental Result

Experiments on MNIST and Fashion-MNIST: We start our experiment by training models using the ten different GANs procedures on **MNIST** and **Fashion-MNIST**. The architecture is DCGAN [32] and the maximum number of epochs is 100.

Figure 3 shows the training curves of the negative critic loss of all candidate approaches. The figure indicates that RWGANs and WGANs are stable with the smallest variances, where RWGANs has a slight higher variance partly due to the use of a larger step-size and asymmetric clamping. This slightly higher variance, nevertheless, speeds up the rate of training. Indeed, as illustrated in Figure 4 and Figure 5, RWGANs is the fastest to generate meaningful images. Note that CGANs and InfoGANs seem faster but the images they have generated are not meaningful, as they fall into bad local optima from an optimization perspective.

Experiments on CIFAR-10 and ImageNet: After observing that WGANs and RWGANs performs the best among all the variants of GANs, we proceed to compare RWGANs and WGANs, together with WGANs with Gradient Penalty (WGANs-GP), on two much larger datasets **CIFAR-10** and **ImageNet**. Here the architectures used are DCGAN and ReLU-MLP [11] and the maximum number of epochs as 25.

⁴<https://github.com/zalando-research/fashion-mnist/>

⁵<https://www.cs.toronto.edu/~kriz/cifar.html>

⁶http://image-net.org/small/train_64x64.tar

Figure 6 shows the training curves of the negative critic loss of all candidate approaches again. Except for the small variance of WGANs, we observe that, in terms of the negative loss, WGANs-GP tend to diverge as the training progresses, implying that such method might not be robust in practice despite its fast rate of training. In this case, RWGANs achieve relatively low variance and convergent negative critic loss, leading to a trade-off between robustness and efficiency.

We then evaluate the candidate methods with the inception score and present the results in Table 2. The table shows that RWGANs are often the fastest method. They perform the best in three out of four cases during several early epochs, and obtain images with competitively high quality at the final stage. Figures 7, Figure 8, Figure 9 and Figure 10 show the sample qualities of the image generated at the initial and final stages, which strongly supports our conclusion.

Architecture	Method	CIFAR-10		ImageNet	
		First 5 epochs	Last 10 epochs	First 3 epochs	Last 5 epochs
DCGAN	RWGANs	1.8606	2.3962	2.0430	2.7008
	WGANs	1.6329	2.4246	2.2070	2.7972
	WGANs-GP	1.7259	2.3731	2.2749	2.7331
MLP	RWGANs	1.3126	2.1710	2.0025	2.4805
	WGANs	1.2798	1.9007	1.7401	2.2304
	WGANs-GP	1.2711	2.2192	1.8845	2.3448

Figure 2: Inception scores at the beginning and final stages of training. DCGAN refers to the standard DCGAN generator and MLP refers to an ReLU-MLP with 4 hidden layers and 512 units at each layer.

5 Conclusion

We propose a novel class of statistical divergence called RW divergence and establish its important theoretical properties, many of which are useful for training GANs. Our numerical experiments have demonstrated promising results of RWGANs parametrized by KL divergence in image generation problems.

Our experiments indicate that asymmetric clamping used in RWGANs approach and gradient penalty used in WGANs-GP are two possible alternatives to alleviate the issues of symmetric clamping in WGANs, which may result in the low-quality samples or the failure of convergence. In addition, asymmetric clamping with larger step-size seems more promising than gradient penalty, which may fail to converge in some settings.

Therefore, RWGANs seem to be a trade-off between WGANs and WGANs-GP, enjoying the low variance of WGANs and the efficiency of WGANs-GP. Compared to the gradient penalty in WGANs-GP, the experiments suggest the potential benefit of larger step-size and flexibility of asymmetric clamping in RWGANs, as indicated theoretically in Lemma 3.4 and Theorem 3.7.

Theoretically, this new conceptual framework under RW provides a unified mathematical framework to

implement and compare different cost functions. The flexibility in RW divergence raises a natural question on how to select the underlying convex function ϕ for a given problem. Empirically, choosing ϕ as the entropy function seems to work reasonably well for image generation problems; however, a more consistent way to select ϕ remains an open problem.

References

- [1] M. Arjovsky, S. Chintala, and L. Bottou. Wasserstein generative adversarial networks. In *ICML*, pages 214–223, 2017.
- [2] Martin Arjovsky and Léon Bottou. Towards principled methods for training generative adversarial networks. *arXiv:1701.04862*, 2017.
- [3] A. Banerjee, X. Guo, and H. Wang. On the optimality of conditional expectation as a Bregman predictor. *IEEE Transactions on Information Theory*, 51(7):2664–2669, 2005.
- [4] A. Banerjee, S. Merugu, I. S. Dhillon, and J. Ghosh. Clustering with Bregman divergences. *Journal of Machine Learning Research*, 6(Oct):1705–1749, 2005.
- [5] D. Berthelot, T. Schumm, and L. Metz. Began: Boundary equilibrium generative adversarial networks. *ArXiv Preprint: 1703.10717*, 2017.
- [6] Y. Brenier. Polar factorization and monotone rearrangement of vector-valued functions. *Communications on Pure and Applied Mathematics*, 44(4):375–417, 1991.
- [7] L. Caffarelli. Some regularity properties of solutions of Monge Ampère equation. *Communications on Pure and Applied Mathematics*, 44(8-9):965–969, 1991.
- [8] L. Caffarelli. The regularity of mappings with a convex potential. *Journal of the American Mathematical Society*, 5(1):99–104, 1992.
- [9] S. Chen and A. Figalli. Partial $W^{2,p}$ regularity for optimal transport maps. *Journal of Functional Analysis*, 272(11):4588–4605, 2017.
- [10] X. Chen, Y. Duan, R. Houthoofd, J. Schulman, I. Sutskever, and P. Abbeel. Infogan: Interpretable representation learning by information maximizing generative adversarial nets. In *NIPS*, pages 2172–2180, 2016.
- [11] B. Conan-Guez and F. Rossi. Multi-Layer Perceptrons for functional data analysis: a projection based approach. *Artificial Neural Networks ICANN 2002*, 2002.
- [12] E. L. Denton, S. Chintala, A. Szlam, and R. Fergus. Deep generative image models using a Laplacian pyramid of adversarial networks. In *NIPS*, pages 1486–1494, 2015.
- [13] L. Evans and R. Gariepy. *Measure Theory and Fine Properties of Functions*. CRC Press, 2015.

- [14] N. Fournier and A. Guillin. On the rate of convergence in Wasserstein distance of the empirical measure. *Probability Theory and Related Fields*, 162(3-4):707–738, 2015.
- [15] A. Ghosh, V. Kulharia, A. Mukerjee, V. Namboodiri, and M. Bansal. Contextual RNN-GANs for abstract reasoning diagram generation. In *AAAI*, pages 1382–1388, 2017.
- [16] I. Goodfellow, J. Pouget-Abadie, M. Mirza, B. Xu, D. Warde-Farley, S. Ozair, A. Courville, and Y. Bengio. Generative adversarial nets. In *NIPS*, pages 2672–2680, 2014.
- [17] I. Gulrajani, F. Ahmed, M. Arjovsky, V. Dumoulin, and A. Courville. Improved training of Wasserstein GANs. In *NIPS*, 2017.
- [18] L. K. Jones and C. L. Byrne. General entropy criteria for inverse problems, with applications to data compression, pattern classification, and cluster analysis. *IEEE Transactions on Information Theory*, 1990.
- [19] D. Kingma and J. Ba. Adam: A method for stochastic optimization. *ArXiv Preprint: 1412.6980*, 2014.
- [20] N. Kodali, J. Abernethy, J. Hays, and Z. Kira. How to train your DRAGAN. *ArXiv Preprint: 1705.07215*, 2017.
- [21] C. Ledig, L. Theis, F. Huszar, J. Caballero, A. P. Aitken, A. Tejani, J. Totz, Z. Wang, and W. Shi. Photo-realistic single image super-resolution using a generative adversarial network. *CoRR*, abs/1609.04802, 2016.
- [22] J. Li, A. Madry, J. Peebles, and L. Schmidt. Towards understanding the dynamics of generative adversarial networks. *arXiv:1706.09884*, 2017.
- [23] P. Luc, C. Couprie, S. Chintala, and J. Verbeek. Semantic segmentation using adversarial networks. In *In NIPS Workshop on Adversarial Training*, 2016.
- [24] X. Ma, N. Trudinger, and X. Wang. Regularity of potential functions of the optimal transportation problem. *Archive for Rational Mechanics and Analysis*, 177(2):151–183, 2005.
- [25] X. Mao, Q. Li, H. Xie, R. Y. K. Lau, Z. Wang, and S. P. Smolley. Least squares generative adversarial networks. *ArXiv Preprint: 1611.04076*, 2016.
- [26] Lars Mescheder, Sebastian Nowozin, and Andreas Geiger. Adversarial variational Bayes: Unifying variational autoencoders and generative adversarial networks. In *ICML*, pages 2391–2400, 2017.
- [27] P. Milgrom and I. Segal. Envelope theorems for arbitrary choice sets. *Econometrica*, 70(2):583–601, 2002.
- [28] M. Mirza and S. Osindero. Conditional generative adversarial nets. *ArXiv Preprint: 1411.1784*, 2014.
- [29] V. Mnih, A. Badia, M. Mirza, A. Graves, T. Lillicrap, T. Harley, D. Silver, and K. Kavukcuoglu. Asynchronous methods for deep reinforcement learning. In *ICML*, pages 1928–1937, 2016.

- [30] A. Odena, C. Olah, and J. Shlens. Conditional image synthesis with auxiliary classifier GANs. In *ICML*, pages 2642–2651, 2017.
- [31] M.C. Pardo and I. Vajda. On asymptotic properties of information-theoretic divergences. *IEEE Transactions on Information Theory*, 49(7):1860–1868, 2003.
- [32] A. Radford, L. Metz, and S. Chintala. Unsupervised representation learning with deep convolutional generative adversarial networks. *Arxiv Preprint: 1511.06434*, 2015.
- [33] S. Reed, Z. Akata, X. Yan, L. Logeswaran, B. Schiele, and H. Lee. Generative adversarial text-to-image synthesis. In *ICML*, pages 1060–1069, 2016.
- [34] T. Salimans, I. Goodfellow, W. Zaremba, V. Cheung, A. Radford, and X. Chen. Improved techniques for training GANs. In *NIPS*, pages 2226–2234, 2016.
- [35] T. Tieleman and G. Hinton. Lecture 6.5-RMSProp: divide the gradient by a running average of its recent magnitude. *COURSERA: Neural Networks for Machine Learning*, 4(2), 2012.
- [36] C. Villani. *Optimal Transport: Old and New*, volume 338. Springer Science & Business Media, 2008.
- [37] C. Vondrick, H. Pirsiavash, and A. Torralba. Generating videos with scene dynamics. In *NIPS*, pages 613–621, 2016.
- [38] R. Yeh, C. Chen, T. Y. Lim, M. Hasegawa-Johnson, and M. N. Do. Semantic image inpainting with perceptual and contextual losses. *ArXiv Preprint: 1607.07539*, 2016.
- [39] J. Zhao, M. Mathieu, and Y. LeCun. Energy-based generative adversarial network. *ArXiv Preprint: 1609.03126*, 2016.
- [40] J.-Y. Zhu, P. Krähenbühl, E. Shechtman, and A. A. Efros. Generative visual manipulation on the natural image manifold. In *ECCV*, pages 597–613, 2016.

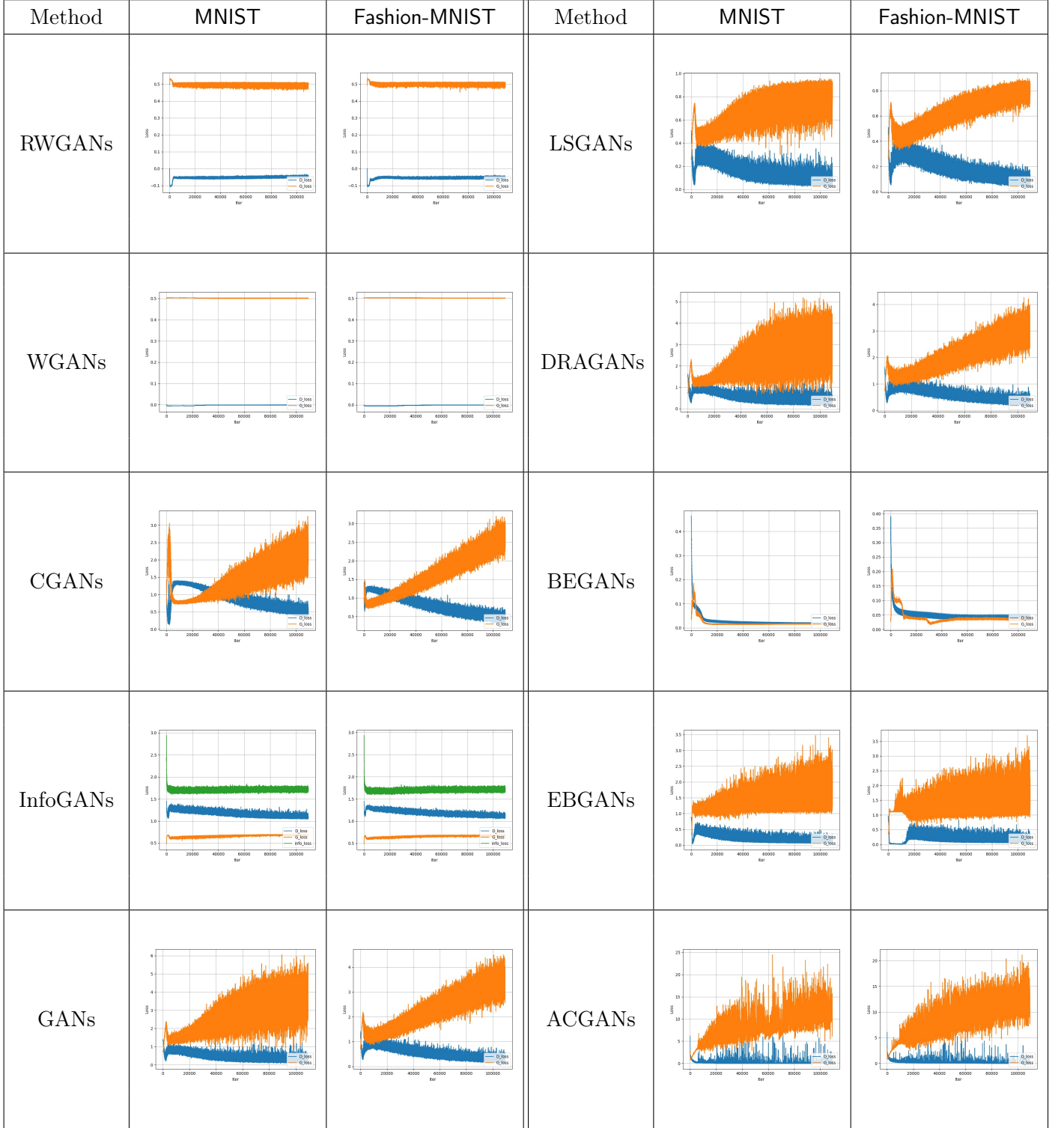




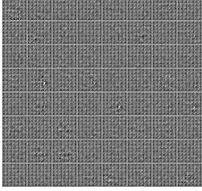
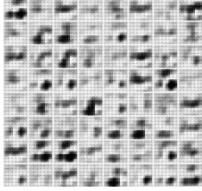






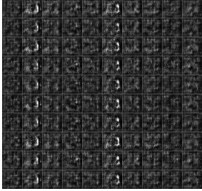



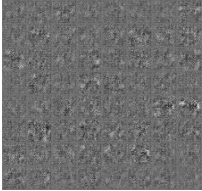





Figure 3: Training curves of the negative critic loss at different stages of training on MNIST and Fashion-MNIST. G_{loss} and D_{loss} refer to the loss in generative and discriminative nets, which is plotted in orange and blue lines, respectively.

Method	$N = 1$	$N = 10$	$N = 25$	$N = 100$
RWGANs				
WGANs				
CGANs				
InfoGANs				
GANs				

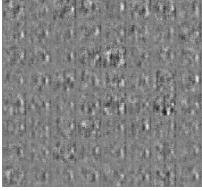



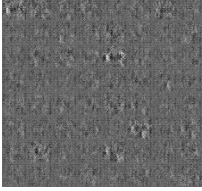



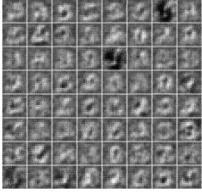



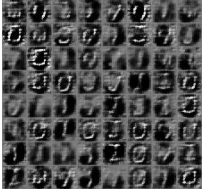



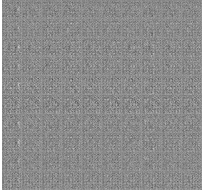
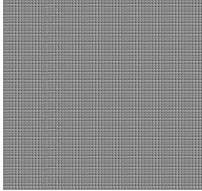
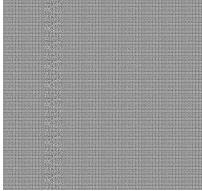
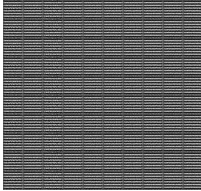
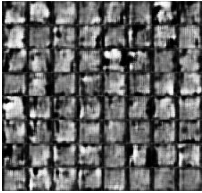



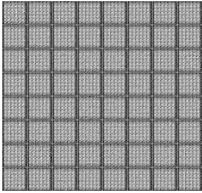
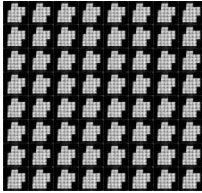
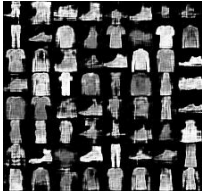


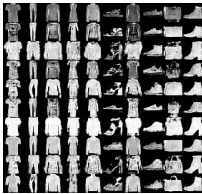
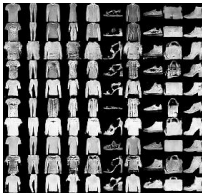
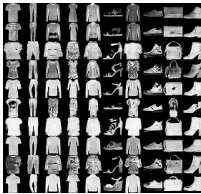
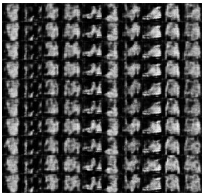
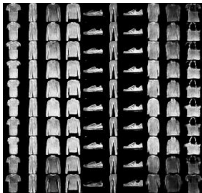
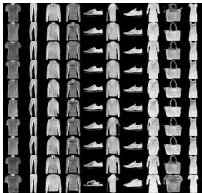
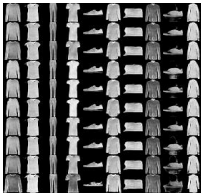
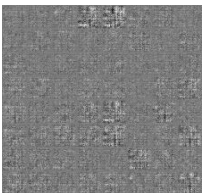
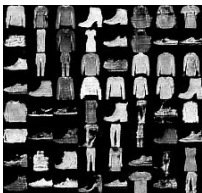


Method	$N = 1$	$N = 10$	$N = 25$	$N = 100$
LSGANs				
DRAGANs				
BEGANs				
EBGANs				
ACGANs				

Figure 4: Sample qualities at different stages of training on MNIST.

Method	$N = 1$	$N = 10$	$N = 25$	$N = 100$
RWGANs				
WGANs				
CGANs				
InfoGANs				
GANs				

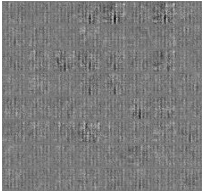
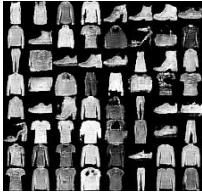


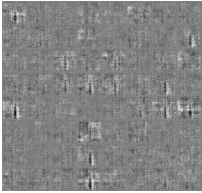



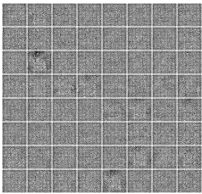
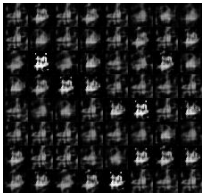

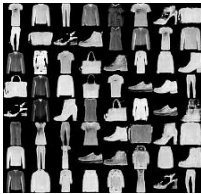
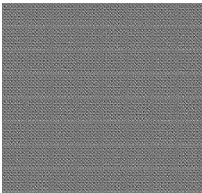
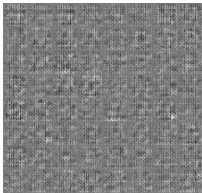

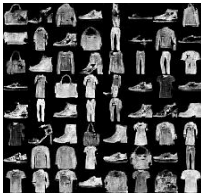
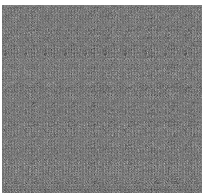
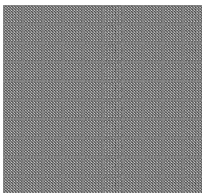
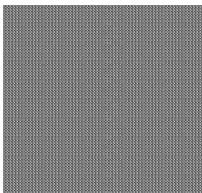
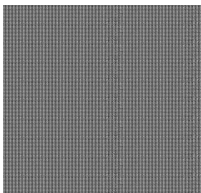
Method	$N = 1$	$N = 10$	$N = 25$	$N = 100$
LSGANs				
DRAGANs				
BEGANs				
EBGANs				
ACGANs				

Figure 5: Sample qualities at different stages of training on Fashion-MNIST.

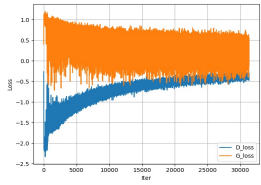
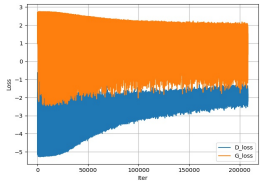
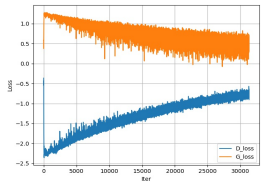
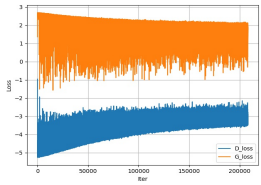
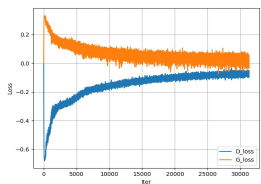
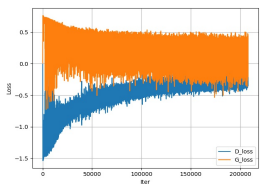
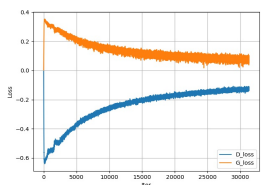
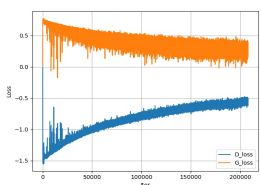
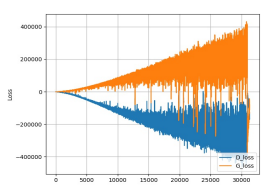
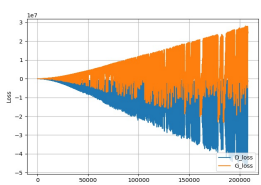
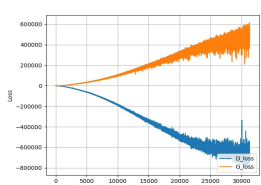
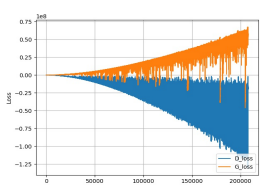
Method	Architecture	CIFAR-10	ImageNet
RWGANs	DCGAN		
	MLP		
WGANs	DCGAN		
	MLP		
WGANs-GP	DCGAN		
	MLP		

Figure 6: Training curves at different stages of training. DCGAN refers to the standard DCGAN generator and MLP refers to an ReLU-MLP with 4 hidden layers and 512 units at each layer. G_{loss} and D_{loss} refer to the loss in generative and discriminative nets. The loss in RWGANs is shown to converge consistently




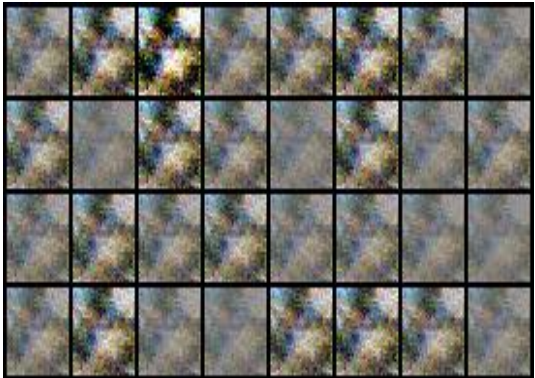

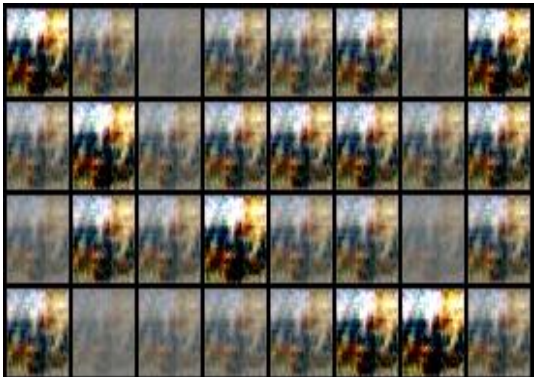
Method	$N = 1$	
	DCGAN	MLP
RWGANs		
WGANs		
WGANs-GP		

Figure 7: Sample qualities at the initial stage of training on CIFAR-10.

Method	$N = 100$	
	DCGAN	MLP
RWGANs		
WGANs		
WGANs-GP		

Figure 8: Sample qualities at the final stage of training on CIFAR-10.





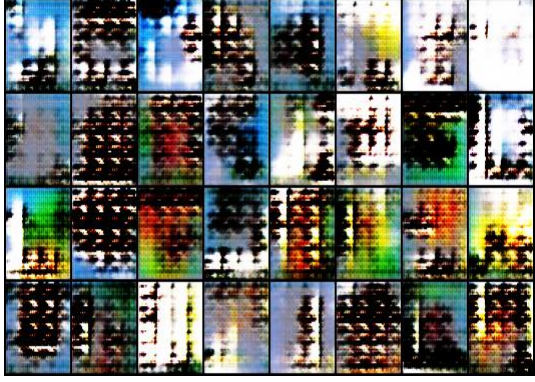

Method	$N = 1$	
	DCGAN	MLP
RWGANs		
WGANs		
WGANs-GP		

Figure 9: Sample qualities at the initial stage of training on ImageNet.

Method	$N = 25$	
	DCGAN	MLP
RWGANs		
WGANs		
WGANs-GP		

Figure 10: Sample qualities at final stage of training on ImageNet.